Ferro-octupolar Order and Low-Energy Excitations in d² Double Perovskites of Osmium

Leonid V. Pourovskii[1,2] Dario Fiore Mosca,[3] and Cesare Franchini[3,4]

[1]*Centre de Physique Théorique, Ecole Polytechnique, CNRS, Institut Polytechnique de Paris, 91128 Palaiseau Cedex, France*
[2]*Collège de France, 11 place Marcelin Berthelot, 75005 Paris, France*
[3]*Faculty of Physics and Center for Computational Materials Science, University of Vienna, Vienna 1090, Austria*
[4]*Department of Physics and Astronomy "Augusto Righi," Alma Mater Studiorum, Università di Bologna, Bologna 40127, Italy*

Conflicting interpretations of experimental data preclude the understanding of the quantum magnetic state of spin-orbit coupled d^2 double perovskites. Whether the ground state is a Janh-Teller–distorted order of quadrupoles or the hitherto elusive octupolar order remains debated. We resolve this uncertainty through direct calculations of all-rank intersite exchange interactions and inelastic neutron scattering cross section for the d^2 double perovskite series Ba_2MOsO_6 ($M =$ Ca, Mg, Zn). Using advanced many-body first-principles methods, we show that the ground state is formed by ferro-ordered octupoles coupled by superexchange interactions within the ground-state E_g doublet. Computed ordering temperature of the single second-order phase transition is consistent with experimentally observed material-dependent trends. Minuscule distortions of the parent cubic structure are shown to qualitatively modify the structure of gaped magnetic excitations.

Identification of complex magnetic orders in spin-orbital entangled and electronically correlated transition metal oxides has emerged as a fascinating field of study, enabling the discovery of new quantum magnetic states originating from interaction between effective pseudospins carrying high-rank multipoles [1,2]. While multipolar coupling in localized f-electron systems has been the subject of intense research and is overall well understood [3,4], the formation and quantum origin of ordered multipoles in d-electron systems is a much more recent research area, which poses challenging issues and controversial opinions [5–9]. Ordered magnetic octupoles were initially proposed as an alternative orbital ordering in e_g manganites arising from the complex mixing of doubly degenerate orbitals [10,11] and later in spin-orbit coupled model systems analogous to Sr_2VO_4, $LiOsO_3$, and $Cd_2Re_2O_7$ [5,6,8]. Rock-salt–ordered double perovskites (DPs) Ba_2MOsO_6 ($M =$ Ca, Mg, Zn; in short, BCOO, BMOO, and BZOO) represent the first candidate materials experimentally proposed to host a d-orbital octupolar order [7]. However, the possibility to actually realize such an exotic magnetic order and the driving mechanism responsible for its formation remain largely debated, in particular, regarding the rank of the multipolar interactions at play, the degree of Janh-Teller (JT) distortions, and the relative importance of direct and indirect exchange [1,7,9,12–14].

In these Os-based DPs, the strong spin-orbit coupling strength splits the effective $L = 1$ t_{2g} levels on the magnetic Os ions into a lower $j = \frac{3}{2}$ quadruplet ground state (GS) and a doublet $j = \frac{1}{2}$ excited state. With a d^2 ($S = 1$)

configuration, the total angular momentum J_{eff} is 2, and the $J_{eff} = 2$ levels are split due to the remnant crystal field (CF) into a lower E_g doublet and T_{2g} triplet [7,15]. In contrast to the assumptions of the pioneering theoretical study of Ref. [15], the intersite exchange interactions are inferred to be much smaller than the remnant CF [7,16]. Despite experimental evidence for a single phase transition involving the E_g manifold [7,17,18], its origin remains unclear.

Considering that the non-Kramers E_g doublet does not carry dipole moments, it would be legitimate to expect that conventional quadrupolar couplings in a JT-broken symmetry would promote an antiferro (AF) quadrupolar order [9,19]. This transparent picture does not seem to be consistent with recent experiments: x-ray diffraction does not find structural distortions (larger than 0.1%) and, whereas no conventional magnetic order is detected by neutron diffraction (upper limit $\approx 0.1~\mu_B$), muon spin relaxation still indicates time-reversal symmetry breaking, thereby ruling out quadrupolar order [18]. To account for the experimental measurements, a ferro-octupolar (FO)-ordered GS was proposed [7,12,13,20], involving a coupling between the lower E_g and excited T_{2g} states mediated by quadrupolar operators. This model reproduces a spin-gap observed in the excitation spectra [7,12] and is overall reasonably compatible with the experimental scenario, but it makes use of some problematic assumptions. Only a subset of intersite exchange interactions (IEIs) allowed within $J_{eff} = 2$ is assumed to be nonzero. Moreover, the included quadrupole IEIs, which cannot be directly inferred from experiment, are tuned to obtain the desired properties of the FO phase.

Inspired by the apparent adequacy of the experimentally proposed FO state and aiming to decipher the key aspects of FO ordering in $5d$-electron systems, we propose in this Letter an alternative mechanism based on direct numerical calculations of all possible interaction channels by means of many-body first-principles schemes. Without forcing any preassumption on the form of the effective Hamiltonian, we find a ferro order of xyz octupoles determined by a competition between time-even and octupolar IEIs within solely the GS E_g doublet. Importantly, employing an analysis that discriminates between direct exchange (DE) and superexchange (SE) mechanisms, we found that IEIs are dominated by SE through O $2p$ and Ba orbitals; $5d$-$5d$ DE contributes only marginally. Our data correctly predict the observed second-order phase transition, with computed ordering temperature compatible with the experimental one and a gapped excitation spectra.

Effective Hamiltonian and methods.—The effective Hamiltonian for the low-energy degrees of freedom on the Os sublattice is a sum of the IEIs (H_{IEI}) and remnant crystal-field (RCF) terms

$$H_{eff} = \sum_{\langle ij \rangle} \sum_{KQK'Q'} V_{KK'}^{QQ'}(\Delta \mathbf{R}_{ij}) O_K^Q(\mathbf{R}_i) O_{K'}^{Q'}(\mathbf{R}_j) + \sum_i H_{RCF}^i,$$

(1)

where the first sum is over all $\langle ij \rangle$ Os–Os bonds, $O_K^Q(\mathbf{R}_i)$ is the Hermitian spherical tensor [4] for $J = 2$ of the rank $K = 1, \ldots, 4$ and projection Q acting on Os site at the position $\mathbf{R}_i$, and the IEI $V_{KK'}^{QQ'}(\Delta \mathbf{R}_{ij})$ acts between the multipoles KQ and $K'Q'$ on two Os sites connected by the lattice vector $\Delta \mathbf{R}_{ij} = \mathbf{R}_j - \mathbf{R}_i$. Finally, $H_{RCF}^i = -V_{RCF}[\mathcal{O}_4^0(\mathbf{R}_i) + 5\mathcal{O}_4^4(\mathbf{R}_i)]$ is the remnant octahedral CF [7], where $\mathcal{O}_K^Q$ are the standard Stevens operators.

To derive the above Hamiltonian, we use density-functional theory (DFT) [21] plus dynamical mean-field theory [22–25], treating the quantum impurity problem on the Os $5d$ shells within the quasiatomic Hubbard-I (HI) approximation [26]. All IEIs $V_{KK'}^{QQ'}(\Delta \mathbf{R})$ are computed within the HI-based force-theorem approach (FT-HI) [27]. Our DFT + HI calculations correctly predict the expected $J_{eff} = 2$ GS multiplet, which is split by H_{RCF} into the ground-state E_g doublet and excited T_{2g} triplet. More details can be found in the Supplemental Material [28].

CF splitting and intersite exchange interactions.—The calculated CF splitting $\Delta_{RCF} = 120V_{RCF}$ listed in Table I is about 20 meV for all members, in agreement with specific heat measurements and excitation gap inelastic neutron scattering (INS) [7,12,16]. The computed IEIs $V_{KK'}^{QQ'}$ are displayed in Fig. 1 (for BZOO, similar data are obtained for the other members, see Supplemental Material [28]). The largest values, ≈ 3 meV, are significantly smaller than Δ_{RCF}, in agreement with experiment [7,12], implying that

TABLE I. Remnant CF splitting Δ_{RCF} and IEIs $J_{\alpha\alpha}$ within the E_g doublet for the Os-Os [1/2,1/2,0] lattice vector. All values are in meV.

Compound	Δ_{RCF}	J_{yy}	J_{zz}	J_{xx}
Ba_2CaOsO_6	17.1	−2.98	1.48	−0.61
Ba_2MgOsO_6	19.2	−2.93	1.67	−0.69
Ba_2ZnOsO_6	20.5	−1.71	1.35	−0.50

the ordered phase will be determined by the IEIs acting within the ground-state E_g doublet.

The E_g space can be encoded by spin-1/2 operators τ_α, with the E_g states corresponding to the projections $\pm 1/2$ of pseudospin-1/2. The resulting E_g Hamiltonian

$$H_{E_g} = \sum_{\langle ij \rangle \in NN} \sum_{\alpha\beta} J_{\alpha\beta}(\Delta \mathbf{R}_{ij}) \tau_\alpha(\mathbf{R}_i) \tau_\beta(\mathbf{R}_j),$$

(2)

is Eq. (1) down-folded into the E_g space (see Supplemental Material [28] for details). Up to a normalization factor, τ_y is the octupole $O_3^{-2} \equiv O_{xyz}$; the corresponding IEI $V_{33}^{\bar{2}\bar{2}}$ directly maps into J_{yy}. τ_x and τ_z are combinations of the e_g quadrupoles (O_2^2 and O_2^0, respectively) with hexadecapoles of the same symmetry. Therefore, V_{22}^{22} and V_{22}^{00} together with the corresponding hexadecapole IEIs contribute to J_{xx} and J_{zz}, respectively. Since the hexadecapole IEIs are negligible, their admixture reduces the magnitude of time-even J_{xx} and J_{zz} (Sec. III in the Supplemental Material [28]). Overall, the order in E_g space is determined by a competition of the time-even (τ_x and τ_z) combinations of quadrupoles and hexadecapoles with the time-odd xyz
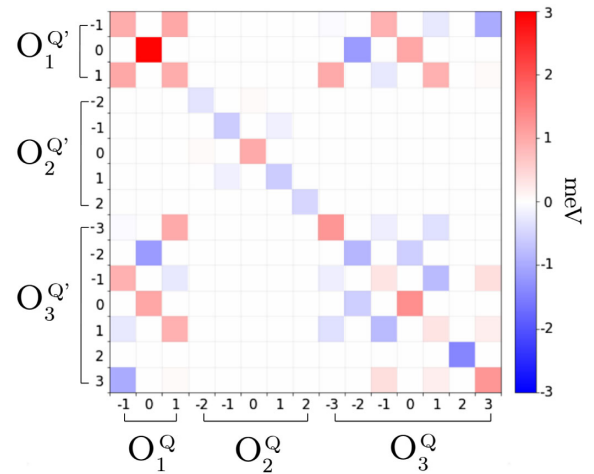
FIG. 1. Color map of the intersite exchange interactions $V_{KK'}^{QQ'}$, Eq. (1), in BZOO for the [1/2,1/2,0] Os-Os pair. The IEIs involving hexadecapoles ($K = 4$) are negligible and not included. The complete list of $V_{KK'}^{QQ'}$ for the three compounds is given in the Supplemental Material [28].

octupole. There are, correspondingly, no IEI coupling τ_y with τ_x or τ_z due to their different symmetry under the time reversal.

Our calculated E_g IEIs for the [1/2,1/2,0] lattice vector are listed in Table I. There are no off-diagonal couplings in this case—only $J_{\alpha\alpha}$ are nonzero. The IEIs for other nearest-neighbor (NN) lattice vectors are obtained by transforming (τ_x, τ_z) with the corresponding rotation matrices of the e_g irreducible representation; J_{yy} is the dominant interaction and, as expected, the same for all the NN bonds; its negative sign corresponds to a ferromagnetic coupling between xyz octupoles, as schematically shown in the inset of Fig. 2. The magnitude of J_{yy} varies substantially between the systems, being about 40% smaller in BZOO as compared to BMOO or BCOO. The IEIs in the time-even (τ_x, τ_y) space are smaller and positive (AF), leading to a possible frustration on the fcc Os sublattice.

We note that our results are qualitatively different from previous assumptions [9,12], since we obtain a significant value for the xyz octupolar IEI $V_{33}^{\bar{2}\bar{2}}$ in the J_{eff} space, see Fig. 1. Since the xyz octupole is directly mapped to τ_y, this results in large J_{yy}. In contrast, Ref. [12] assumed zero $V_{33}^{\bar{2}\bar{2}}$; to obtain a reasonable value for effective J_{yy} through an "excitonic" mechanism, a huge quadrupole IEI $V_{xy-xy} \equiv V_{22}^{\bar{2}\bar{2}} \sim 35$ meV (in our spherical tensor normalization) was employed, which is about 2 orders of magnitude larger than the one predicted by our calculations (see Fig. 1 and Supplemental Material [28]). Reference [9] considered only Os-Os DE and found the J_{yy} IEI to be zero.

In order to discriminate between DE and various SE contributions to the IEIs, we have developed an approach to exclude a chosen set of hopping processes from IEIs.
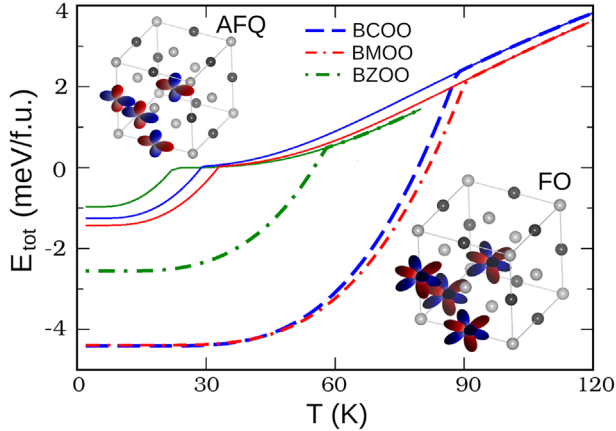
FIG. 2. Mean-field total energy vs temperature calculated from the Hamiltonian (1), with the zero energy corresponding to the ground-state energy of H_{RCF} (E_g doublet). The bold lines are the energies calculated from the full Hamiltonian. The thin solid lines of the corresponding colors are calculated with the IEIs between xyz octupoles set to zero. The insets depict the resulting FO and AF quadrupolar (AFQ) orders.

This approach is based on expanding the down-folded Os $5d$ orbitals onto a set of all relevant valence states (Ref. [42], see Supplemental Material [28] for details). This analysis shows that the effect of Os-Os DE is insignificant (below 10%). The IEIs are dominated by SE processes, involving hoppings through O $2p$ and Ba states (Supplemental Material, Table II [28]), with contributions of similar magnitude to both quadrupolar and octupolar IEIs. These results explain the comparable strength of quadrupolar and octupolar IEIs in the $J_{\text{eff}} = 2$ space (Fig. 1 and Supplemental Material [28]). The time-even IEIs in the E_g space are then further diminished by the hexadecapoles admixture into τ_x and τ_z as discussed above, resulting in a dominating xyz coupling J_{yy} (Table I).

A dominating SE also naturally explains the weaker IEIs in BZOO as compared to two other systems. Substituting Mg or Ca at the M site by more electronegative Zn results in a more covalent M–O bond that weakens the Os–O bond through "covalency competition" [43]. As a result, the principal Os-Os SE coupling through O and Ba is reduced.

Ordered phase.—From the first-principles effective Hamiltonian (1), we evaluate the ordered phases and transition temperatures T_o within the mean-field approximation (MFA) [44]. All three systems exhibit a single second-order phase transition into the FO xyz phase, as shown in Fig. 2 where the zero-T limit corresponds to the FO ground-state ordering energy. The only nonzero $J_{\text{eff}} = 2$ multipoles at the FO ground state are $\langle O_{xyz} \rangle$ (fully saturated at $1/\sqrt{2}$ for the spherical tensor normalization) as well as the "40" and "44" hexadecapoles arising due to H_{RCF} and exhibiting no peculiarity at T_o. The quasilinear behavior of E_{tot} above the T_o is due to the CF term. The calculated values of the FO T_o (T_o^{FO} in Table II) systematically overestimate the experimental one by about 80% due to the employed approximations (MFA and HI), in line with previous applications of the FT-HI framework [45–47], but the material-dependent changes are captured very well ($T_o^{\text{FO}_{\text{BCOO}}}/T_o^{\text{FO}_{\text{BZOO}}} \approx 1.6$, while $T_o^{\text{FO}_{\text{BCOO}}}/T_o^{\text{FO}_{\text{BMOO}}} \approx 1$).

To explore competing time-even orders, we set the xyz IEI to zero and obtain a planar AF order of the e_g quadrupoles and associated hexadecapoles, with ferroalignment of all order parameters (encoded by $\langle \tau_x \rangle$ and $\langle \tau_z \rangle$) within (001) planes that are AF stacked in the [001]

TABLE II. Calculated mean-field ordering temperatures T_o (in kelvin) for the FO xyz and time-even AF phases compared to the experimental values from Refs. [17,18]. Last two columns: the energies (in meV) of the singlet (E_S) and triplet (E_T) excited levels of the $J_{\text{eff}} = 2$ multiplet in the FO xyz ground state.

Compound	T_o^{FO}	T_o^{AF}	T_o^{exp}	E_S	E_T
Ba_2CaOsO_6	89	29	49	17.7	25.9
Ba_2MgOsO_6	91	33	51	17.6	28.0
Ba_2ZnOsO_6	58	23	30	10.2	25.6

direction. This structure (shown as the inset in Fig. 2, as well as in the Supplemental Material [28]) is in agreement with the quadrupolar order previously predicted by Ref. [9]. The corresponding ordering temperature T_o^{AF} is about 3 times smaller than T_o^{FO} (see Fig. 2 and Table II). Considering that this AF order in the cubic phase is unstable against JT distortions [9], the release of JT modes is expected to further stabilize the AF phase, but most unlikely by a factor of 3. No sign of JT distortions above 0.1% have been measured in BCOO [7].

Generalized susceptibility and on-site excitations.— Information on the characteristic excitations of the FO *xyz* order is encoded in generalized dynamical lattice [$\chi(\mathbf{q}, E)$] and single-site [$\chi_0(E)$] susceptibility, which we computed within the random phase approximation (RPA) (see Ref. [48] and Supplemental Material [28]). The matrix elements $\chi_0^{\mu\mu'}(E)$ are evaluated from the eigenvalues E and eigenstates Ψ of the $J_{eff} = 2$ manifold,

$$\chi_0^{\mu\mu'}(E) = \sum_{AB} \frac{\langle \Psi_A | O_\mu | \Psi_B \rangle \langle \Psi_B | O_{\mu'} | \Psi_A \rangle}{E_B - E_A - E} [p_A - p_B], \quad (3)$$

where $A(B)$ labels five single-site eigenvalues and eigenstates of the Hamiltonian (1), the combined index $\mu = [K, Q]$ labels J_{eff} multipoles, and $p_{A(B)}$ is the corresponding Boltzmann weight.

In the FO GS, the $J_{eff} = 2$ manifold is split into three levels (Table II): singlet GS, first singlet (S) excited state (with opposite sign of *xyz* octupole compared to GS and energy proportional to IEIs), and a high-energy T_{2g} triplet (T) due to Δ_{RCF} further enhanced by IEIs (cf. Table I). In contrast to the E_g doublet, the T_{2g} triplet degeneracy is not lifted by the *xyz* exchange field, since the direct product $T_{2g} \times T_{2g}$ does not contain the irreducible representation A_{2u} of the *xyz* octupole.

We find that only e_g quadrupoles and hexadecapoles connect the GS with the first excited S state, and since the IEI matrices do not couple time-odd and time-even multipoles, this S excitation can induce only time-even contributions to the RPA lattice susceptibility $\chi(\mathbf{q}, E)$. In contrast, the matrix elements $\langle \Psi_{GS} | O_\mu | \Psi_T \rangle$ between GS and T levels take nonzero values for many odd and even multipoles [see inset in Fig. 3(a)].

Inelastic neutron-scattering cross section.—To provide further evidence directly comparable with available measurements [7], from the knowledge of $\chi(\mathbf{q}, E)$ we compute the magnetic contribution to the INS differential cross section,

$$\frac{d^2\sigma}{d\Omega dE'} \propto \sum_{\alpha\beta} (\delta_{\alpha\beta} - q_\alpha q_\beta)$$
$$\times \left[\sum_{\mu\mu'} F_{\alpha\mu}(\mathbf{q}) F_{\beta\mu'}(\mathbf{q}) \text{Im} \chi_{\mu\mu'}(\mathbf{q}, E) \right], \quad (4)$$

where we drop unimportant prefactors. In order to take into account the octupole contributions into the INS cross sections, the form factors $F_{\alpha\mu}(\mathbf{q})$ are evaluated beyond the dipole approximation on the basis of Refs. [49,50] (for more details, see the Supplemental Material [28]).

The calculated powder-averaged (averaged over $\mathbf{q}$ directions) INS cross section for BZOO is displayed in Fig. 3(a) (similar results for BCOO and BMOO are given in the Supplemental Material [28]). One clearly observes a band of CF excitations above 20 meV, in agreement with the magnitude of E_T. However, below the CF band one sees no features corresponding to transitions to the lower-energy S
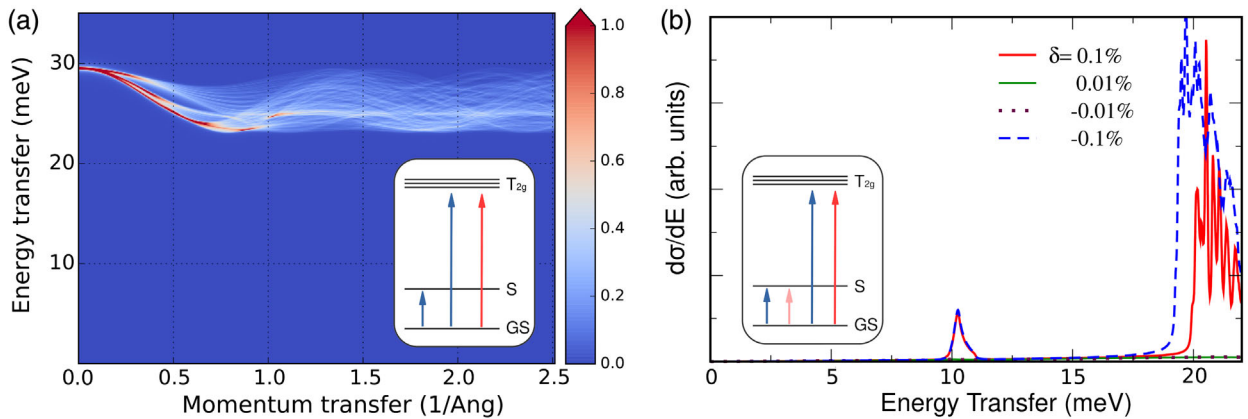
FIG. 3. (a) Color map of the calculated powder-averaged INS differential cross section in cubic BZOO as a function of the energy transfer E and momentum transfer q. Inset: on-site splitting of $J_{eff} = 2$ levels in the ferro-octupolar phase. Allowed time-even and time-odd transitions between the levels are schematically shown by blue and red arrows, respectively. (b) q-integrated INS differential cross section of BZOO for the tetragonal distortions $\delta = \pm 0.1\%$ and $\pm 0.01\%$. An exchange peak at about 10 meV is clearly seen for the larger distortion. The onset of crystal-field excitations is seen above 18–20 meV. Inset: the corresponding $J_{eff} = 2$ level scheme with a time-odd (*xyz*) transition (pale red arrow) between the ground-state and singlet levels turned on by the distortions.

excitation. As only odd-time multipoles contribute to the magnetic neutron scattering, this result can be anticipated from the structure of on-site excitations in the FO xyz phase.

We conclude by showing the effect of minuscule tetragonal distortions δ on the INS spectrum. The remnant CF potential acting on the $J_{\mathrm{eff}} = 2$ multiplet in the distorted structure becomes $H^i_{\mathrm{RCF}} = -V_{\mathrm{RCF}}[\mathcal{O}^0_4(\mathbf{R}_i) + 5\mathcal{O}^4_4(\mathbf{R}_i)] + V_t \mathcal{O}^0_2(\mathbf{R}_i)$, where the tetragonal contribution $V_t = K_t \delta$. Using BZOO as case material, we perform a series of DFT + HI calculations for tetragonally distorted BZOO for δ in the range of -0.5%–0.5% extracting $K_t = 266$ meV (see Supplemental Material [28]). Then, we add $\sum_i K_t \delta \mathcal{O}^0_2(\mathbf{R}_i)$ to the Hamiltonian (1) and solve it in the MFA for small values of δ up to 0.1%. We observe the same transition into the FO xyz order with T_o about 58 K, as in the initial case. The only difference is that $\langle O_{z^2} \rangle$ is nonzero, reaching about 1/4 of its saturated value for $\delta = 0.1\%$ and an order of magnitude less for $\delta = 0.01\%$. In the case of tetragonal compression ($\delta < 0$) we obtain the same $\langle O_{z^2} \rangle$ magnitudes with opposite sign. The important point is that the GS and excited singlet Ψ_S now feature a nonzero matrix element for the time-odd xyz, $\langle \Psi_{\mathrm{GS}} | O_{xyz} | \Psi_S \rangle \propto \langle O_{z^2} \rangle_{\mathrm{GS}}$. Therefore, magnetic excitations across the gap become possible [see inset in Fig. 3(b)] and should be, in principle, visible by INS.

We evaluated the powder-averaged INS cross section for a set of small distortions ($\delta = \pm 0.1\%$ and $\delta = \pm 0.01\%$). We then integrate $\{[\delta^2\sigma(q,\omega)]/(d\Omega dE')\}$ over the same range of q and E as the experimental INS spectra (Fig. 1 in Ref. [7]). In the resulting cross section shown in Fig. 3(b) the contribution of magnetic scattering across the exchange gap is completely negligible for $\delta = \pm 0.01\%$. For the larger distortion ($\delta = \pm 0.1\%$), a narrow peak emerges at $E \approx 10$ meV, also visible in experimental INS data [7]. This peak has a small, but not negligible intensity as compared to the crystal-field excitations. The onset of the latter is shifting below 20 meV with increasing distortions [Fig. 3(b)].

Conclusions.—Our first-principles calculations provide robust qualitative and quantitative evidence of a purely ferro order of xyz octupoles in d^2 DPs [7,12,51], determined by a competition between the time-even and octupolar IEIs within the ground-state E_g doublet, alternative to previous models based on unrealistically large quadrupolar coupling. Our study reveals the role of superexchange as the main mechanism for triggering the formation of octupolar ordering in spin-orbit coupled 5d oxides. The obtained ordering temperatures are consistent with material-dependent trends. The simulated INS spectrum correctly reproduces the CF excitations in the cubic phase, and small tetragonal distortions are necessary to activate the O_{xyz} octupole operator connecting the exchange-split ground and first excited states to generate the measured exchange peak [7].

[1] T. Takayama, J. Chaloupka, A. Smerald, G. Khaliullin, and H. Takagi, J. Phys. Soc. Jpn. **90**, 062001 (2021).

[2] W. Witczak-Krempa, G. Chen, Y. B. Kim, and L. Balents, Annu. Rev. Condens. Matter Phys. **5**, 57 (2014).

[3] Y. Kuramoto, Prog. Theor. Phys. Suppl. **176**, 77 (2008).

[4] P. Santini, S. Carretta, G. Amoretti, R. Caciuffo, N. Magnani, and G. H. Lander, Rev. Mod. Phys. **81**, 807 (2009).

[5] L. Fu, Phys. Rev. Lett. **115**, 026401 (2015).

[6] G. Jackeli and G. Khaliullin, Phys. Rev. Lett. **103**, 067205 (2009).

[7] D. D. Maharaj, G. Sala, M. B. Stone, E. Kermarrec, C. Ritter, F. Fauth, C. A. Marjerrison, J. E. Greedan, A. Paramekanti, and B. D. Gaulin, Phys. Rev. Lett. **124**, 087206 (2020).

[8] J. W. Harter, Z. Y. Zhao, J.-Q. Yan, D. G. Mandrus, and D. Hsieh, Science **356**, 295 (2017).

[9] G. Khaliullin, D. Churchill, P. P. Stavropoulos, and H.-Y. Kee, Phys. Rev. Research **3**, 033163 (2021).

[10] A. Takahashi and H. Shiba, J. Phys. Soc. Jpn. **69**, 3328 (2000).

[11] J. van den Brink and D. Khomskii, Phys. Rev. B **63**, 140416(R) (2001).

[12] A. Paramekanti, D. D. Maharaj, and B. D. Gaulin, Phys. Rev. B **101**, 054439 (2020).

[13] S. Voleti, D. D. Maharaj, B. D. Gaulin, G. Luke, and A. Paramekanti, Phys. Rev. B **101**, 155118 (2020).

[14] S. W. Lovesey and D. D. Khalyavin, Phys. Rev. B **102**, 064407 (2020).

[15] G. Chen and L. Balents, Phys. Rev. B **84**, 094420 (2011).

[16] K. Yamamura, M. Wakeshima, and Y. Hinatsu, J. Solid State Chem. **179**, 605 (2006).

[17] C. M. Thompson, J. P. Carlo, R. Flacau, T. Aharen, I. A. Leahy, J. R. Pollichemi, T. J. S. Munsie, T. Medina, G. M. Luke, J. Munevar, S. Cheung, T. Goko, Y. J. Uemura, and J. E. Greedan, J. Phys. Condens. Matter **26**, 306003 (2014).

[18] C. A. Marjerrison, C. M. Thompson, A. Z. Sharma, A. M. Hallas, M. N. Wilson, T. J. S. Munsie, R. Flacau, C. R. Wiebe, B. D. Gaulin, G. M. Luke, and J. E. Greedan, Phys. Rev. B **94**, 134429 (2016).

[19] D. Churchill and H.-Y. Kee, arXiv:2109.08104.

[20] S. Voleti, A. Haldar, and A. Paramekanti, arXiv:2109.13266.

[21] P. Blaha, K. Schwarz, G. Madsen, D. Kvasnicka, J. Luitz, R. Laskowski, F. Tran, and L. D. Marks, *WIEN2k, An Augmented Plane Wave + Local Orbitals Program for Calculating Crystal Properties* (Karlheinz Schwarz, Technische Universität Wien, Austria, 2018), ISBN 3-9501031-1-2.

[22] A. Georges, G. Kotliar, W. Krauth, and M. J. Rozenberg, Rev. Mod. Phys. **68**, 13 (1996).

[23] V. I. Anisimov, A. I. Poteryaev, M. A. Korotin, A. O. Anokhin, and G. Kotliar, J. Phys. Condens. Matter **9**, 7359 (1997).

[24] A. I. Lichtenstein and M. I. Katsnelson, Phys. Rev. B **57**, 6884 (1998).

[25] M. Aichhorn, L. Pourovskii, P. Seth, V. Vildosola, M. Zingl, O. E. Peil, X. Deng, J. Mravlje, G. J. Kraberger, C. Martins *et al.*, Comput. Phys. Commun. **204**, 200 (2016).

[26] J. Hubbard, Proc. R. Soc. A **276**, 238 (1963).

[27] L. V. Pourovskii, Phys. Rev. B **94**, 115117 (2016).

[28] See Supplemental Material at http://link.aps.org/supplemental/10.1103/PhysRevLett.127.237201 for derivations, detailed methodology and additional data, which includes Refs. [29–41].

[29] M. Aichhorn, L. Pourovskii, V. Vildosola, M. Ferrero, O. Parcollet, T. Miyake, A. Georges, and S. Biermann, Phys. Rev. B **80**, 085101 (2009).

[30] M. Aichhorn, L. Pourovskii, and A. Georges, Phys. Rev. B **84**, 054529 (2011).

[31] V. I. Anisimov, I. V. Solovyev, M. A. Korotin, M. T. Czyżyk, and G. A. Sawatzky, Phys. Rev. B **48**, 16929 (1993).

[32] D. Fiore Mosca, L. V. Pourovskii, B. H. Kim, P. Liu, S. Sanna, F. Boscherini, S. Khmelevskyi, and C. Franchini, Phys. Rev. B **103**, 104401 (2021).

[33] A. S. Erickson, S. Misra, G. J. Miller, R. R. Gupta, Z. Schlesinger, W. A. Harrison, J. M. Kim, and I. R. Fisher, Phys. Rev. Lett. **99**, 016404 (2007).

[34] A. Georges, L. d. Medici, and J. Mravlje, Annu. Rev. Condens. Matter Phys. **4**, 137 (2013).

[35] S. M. Winter, Y. Li, H. O. Jeschke, and R. Valentí, Phys. Rev. B **93**, 214431 (2016).

[36] A. E. Taylor, S. Calder, R. Morrow, H. L. Feng, M. H. Upton, M. D. Lumsden, K. Yamaura, P. M. Woodward, and A. D. Christianson, Phys. Rev. Lett. **118**, 207202 (2017).

[37] B. Yuan, J. P. Clancy, A. M. Cook, C. M. Thompson, J. Greedan, G. Cao, B. C. Jeon, T. W. Noh, M. H. Upton, D. Casa, T. Gog, A. Paramekanti, and Y.-J. Kim, Phys. Rev. B **95**, 235114 (2017).

[38] K. Kobayashi, T. Nagao, and M. Ito, Acta Crystallogr. Sect. A **67**, 473 (2011).

[39] C. Stassis and H. W. Deckman, J. Phys. C **9**, 2241 (1976).

[40] L. V. Pourovskii, J. Boust, R. Ballou, G. G. Eslava, and D. Givord, Phys. Rev. B **101**, 214433 (2020).

[41] B. Amadon, F. Lechermann, A. Georges, F. Jollet, T. O. Wehling, and A. I. Lichtenstein, Phys. Rev. B **77**, 205112 (2008).

[42] P. Delange, S. Biermann, T. Miyake, and L. Pourovskii, Phys. Rev. B **96**, 155132 (2017).

[43] I. Yamada, A. Takamatsu, N. Hayashi, and H. Ikeno, Inorg. Chem. **56**, 9303 (2017).

[44] M. Rotter, J. Magn. Magn. Mater. **272–276**, E481 (2004).

[45] A. Horvat, L. Pourovskii, M. Aichhorn, and J. Mravlje, Phys. Rev. B **95**, 205115 (2017).

[46] L. V. Pourovskii and S. Khmelevskyi, Phys. Rev. B **99**, 094439 (2019).

[47] L. V. Pourovskii and S. Khmelevskyi, Proc. Natl. Acad. Sci. U.S.A. **118**, e2025317118 (2021).

[48] J. Jensen and A. R. Mackintosh, *Rare Earth Magnetism: Structures and Excitations* (Clarendon Press, Oxford, 1991).

[49] R. Shiina, O. Sakai, and H. Shiba, J. Phys. Soc. Jpn. **76**, 094702 (2007).

[50] S. W. Lovesey, *Theory of Neutron Scattering from Condensed Matter* (Clarendon Press, Oxford, 1984).

[51] S. W. Lovesey and D. D. Khalyavin, Phys. Rev. B **102**, 064407 (2020).